High-temperature superelasticity of $Ni_{50.6}Ti_{24.4}Hf_{25.0}$ shape memory alloy

Luca Patriarca* and Huseyin Sehitoglu

Department of Mechanical Science and Engineering, University of Illinois at Urbana–Champaign, 1206 W. Green St., Urbana, IL 61801, USA

Received 11 August 2014; revised 17 November 2014; accepted 11 January 2015
Available online 23 January 2015

There is remarkable interest in ternary NiTi-based shape memory alloys (SMAs) for high-temperature applications [1]. The addition of a ternary element (Hf, Zr, Pd, Pt, and Au) increases the transformation temperatures extending the use of NiTi-based SMAs to high temperatures (above 100 °C). Among the potential ternary alloying elements, Zr and Hf are the most attractive candidates due to their low price compared to others. In particular, Hf is generally preferred to Zr for two reasons. First of all at the same concentrations, the transformation temperatures are higher in the case of Hf addition. Secondly, the addition of Hf leads to higher transformation strains which are preferred for industrial applications (e.g. in actuators). While more work has been done for NiTiHf SMAs with Hf content lower than 20 at.%, much less interest has been dedicated to higher Hf content (>20%). In this paper we present a preliminary study on the $Ni_{50.6}Ti_{24.4}Hf_{25.0}$ alloy focusing on the specific aging treatments which lead to the high temperature shape memory and superelastic behaviors.

Since its early appearance [2], the addition of Hf in NiTi-based shape memory alloys has attracted researchers as the transformation temperatures are easily increased from approximately 100 °C (NiTi alloys) up to 600 °C (addition of Hf 30 at.%) for near-equiatomic Ni content (50 at.%) [3]. Though such high temperatures are undoubtedly desirable for industrial applications, high Hf percentages are generally detrimental for some important mechanical characteristics, i.e. ductility [1]. Researchers were then encouraged to work with typical Hf concentrations from 15% to 20%, while less interest has been dedicated to lower Hf levels [4–6] since the low increment of the transformation temper-atures. Different research studies have been dedicated to the $NiTiHf_{15}$ alloy [7–11], and many others to the $NiTiHf_{20}$ alloy [12–20]. On the other hand, very few works have been published on NiTiHf alloys with Hf concentrations higher than 20%. However, the few results published confirm that the transformation temperatures are further increased [3,21–23], and that these alloys are worth to be investigated. Transformation temperatures and the mechanical behavior of NiTiHf alloys can also be improved by cold rolling + annealing, and aging. While cold rolling is not desirable for the industrial applications, Meng. and coworkers [18] have shown that with a proper precipitation induced by aging, the shape memory properties and the strength of the NiTiHf alloys can be further improved and stabilized. Several studies have successfully demonstrated the effect of the precipitation process on the functional behavior of the nickel-rich NiTiHf alloys, in particular focusing on the isobaric/isothermal shape memory and superelastic behaviors. Perfect superelasticity in $NiTiHf_{20}$ was discovered at high temperatures: at 210 °C by Coughlin et al. [14], at 220 °C by Bigelow et al., and at 240 °C by Benafan et al. [24] and Karaca et al. [16]. In this paper we investigate the shape memory and pseudo-elastic behavior of the $Ni_{50.6}Ti_{34.4}Hf_{25.0}$ alloy which has not yet been explored. Transformation temperatures have been determined for a wide range of aging temperatures and times. Contrary to other studies, no hot/cold extrusion was adopted for improving shape memory and pseudoelastic behaviors. Moreover, using high resolution strain mea-surements via Digital Image Correlation (DIC) technique we provide the stress–strain behavior in compression

* Corresponding author. Tel.: +1 217 333 3859.; e-mail: patriarc@illinois.edu

showing perfect high temperature superelastic behavior up to 300 °C.

The new high-temperature shape memory alloy with a target composition of $Ni_{50.6}Ti_{34.4}Hf_{25.0}$ (at.%) was produced by plasma melting. The ingots were successively sectioned into 4 mm × 4 mm × 10 mm compression specimen by electro-discharged machining. The average grain size was measured as approximately 300 μm. Specimens were homogenized at 1000 °C for 4 h under vacuum and then slowly cooled into the furnace. Some of the specimens were further cut using a low speed diamond saw into small flat pieces with an average weight of 40–50 mgr suited for Differential Scanning Calorimetry (DSC) measurements. All homogenized specimens were successively solution-treated for 1 h at 900 °C and then quenched into iced water. DSC specimens were aged at temperatures ranging from 400 °C and 700 °C, and for different aging times from 1 h to 12 h. All DSC samples were successively polished using SiC paper in order to remove the thin oxidized layer formed after solutionizing and aging treatments. Transformation temperatures were determined using a Perking Elmer Pyris 1 differential scanning calorimeter with a heating/cooling rate of 40 °C/min. Heat flow data were obtained from room temperature up to 500 °C. The transformation temperatures are herein indicated as the Austenite peak temperature (A_{PT}) and the Martensite peak temperature (M_{PT}).

The isothermal compression experiments were conducted using an MTS servo hydraulic load frame. Specimens were deformed in displacement control at an average strain rate of 10^{-4} s^{-1}. A Lepel induction generator and an induction coil were used to heat the compression grips. The temperature of the specimen was measured with a Raytek infrared temperature sensor. Strain data for constructing the stress–strain curves were obtained with in situ DIC. Images were captured using an IMI model IMB-202 FT CCD camera (1600 × 1200 pixels) with a Navitar optical lens, providing a resolution of 3.0 μm/pixel. The speckle pattern for DIC was obtained using black paint and an Iwata Micron B airbrush. Prior to load, all specimens were heated and held for 30 min at the maximum temperature (approximately A_{PT} +70 °C) in order to stabilize the speckle pattern and complete the Martensite-to-Austenite phase transformation. The test temperature was successively reached by slowly cooling the specimen from A_{PT} +70 °C. At the selected temperature, a reference image of the sample surface was captured at zero stress, and the deformed images of the same area every 2 s during loading. Images were successively correlated and the axial strains were used to construct the stress–strain curves.

The most important DSC curves are shown in Figure 1. After homogenization, the $Ni_{50.6}Ti_{34.4}Hf_{25.0}$ alloy shows the higher A_{PT} and M_{PT} compared to other aging temperatures and time combination adopted in this study. Precipitation occurs during the slow cooling from 1000 °C to room temperature and moves the A_{PT} and M_{PT} to high temperatures, respectively 354 °C and 288 °C. For the solution-treated case the transformation temperatures decrease to $A_{PT} = 255$ °C and $M_{PT} = 204$ °C leading to a peak-to-peak temperature difference of $(A_{PT}-M_{PT})_{Hom} = 66$ °C and $(A_{PT}-M_{PT})_{Sol} = 51$ °C. The aging between 400 °C and 500 °C for 1 h further decreases the A_{PT}, meanwhile the M_{PT} shows a different trend which causes the $(A_{PT}-M_{PT})$ to have a maximum between the two aging temperatures. Increasing the aging temperature (>500 °C) moves the transformation temperatures close to the

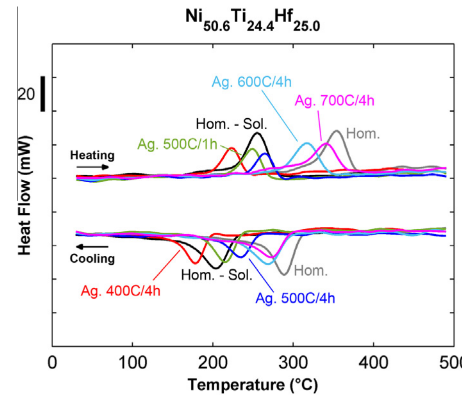

Figure 1. DSC curves showing the effect of aging on the transformation temperatures for the $Ni_{50.6}Ti_{24.4}Hf_{25.0}$ alloy. Depending on the aging treatment (temperature and time), the transformation temperatures can increase or decrease than the solution-treated case.

homogenized case. It is worthwhile to remark that during the slow cooling following homogenization (2 °C/min), the sample remains for sufficient time in the temperature interval (400–500 °C) which, for the solution-treated case, decreases the transition temperatures. Since the transition temperatures between the homogenized case and the 700 °C/4 h aging case are not significantly different, we can conclude that aging at very high temperatures also stabilizes the transition temperatures.

Figure 2 shows a summary of the most important DSC data acquired in this study for the aged samples after analyzing approx. 30 combinations of aging temperature and time. For the 500 °C/4 h aging we found a minimum in the peak-to-peak difference $(A_{PT}-M_{PT})_{500°C/4h} = 29$ °C. For the same temperature, a shorter aging time produces lower A_{TP} and M_{TP} temperatures but a peak-to-peak difference similar to the 4 h aging time $(A_{PT}-M_{PT})_{500°C/1h} = 31$ °C. Decreasing the aging temperature from 500 °C to 400 °C (at the fixed aging time of 1 h), the A_{PT} slowly decreases, while the M_{PT} shows a minimum between 500 °C and 400 °C. At aging temperatures higher than 500 °C the A_{PT} increases faster than the M_{PT} producing an increment of the $(A_{PT}-M_{PT})$ difference. A further increase in the aging time (12 h at 650 °C) does not provide a significant increment of the transformation temperatures.

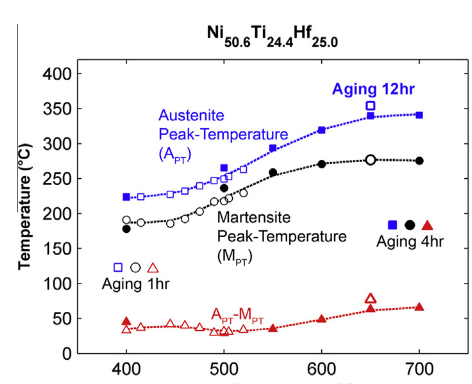

Figure 2. Effect of the aging temperature and time on the Martensite and Austenite peaks temperatures (M_{PT}, A_{PT}). Transformation temperatures and peak-to-peak difference $(A_{PT}-M_{PT})$ both increase with aging temperature and time above 500 °C aging temperature.

Stress–strain curves obtained for the $Ni_{50.6}Ti_{34.4}Hf_{25.0}$ alloy are illustrated in Figure 3. The black stress–strain curves are calculated averaging the axial strain over the entire DIC region (3.8 mm × 2.6 mm) of the specimen's surface, while the blue curves refer to local strain measurements obtained averaging the axial strains in the DIC sub-region of the maximum local strain. Local strain measurements indicate the region of the specimen where locally a large region is subjected to the reversible martensite transformation. For the solution-treated specimen, the initial test temperatures (205 ° C and 220 ° C) were chosen across the M_S temperature. In these cases the total deformation can be subdivided into three components: elastic deforma-tion, stress-induced martensitic transformation of the aus-tenite, and deformation of the martensite. Elastic deformation and the stress-induced martensitic transforma-tion are recovered upon unloading (superelasticity, SE), while the strain component due to the martensite deforma-tion is recovered upon heating the unstressed specimen (shape memory SM, Fig. 3). The solution-treated case shows almost perfect pseudoelastic behavior in the range of temperatures (230 ° C–260 ° C). Locally, the measured strains are higher: at 245 ° C the average strain measured over the entire DIC region is $\bar{\varepsilon} = 1.93\%$ and negligible residual strains, while locally we measured an average local strain of $\varepsilon_{loc} = 2.74\%$ and a residual strain of $\varepsilon^{res}{}_{loc} = 0.28\%$. Aging at 500 ° C for 4 h results in an excellent superelas-tic behavior up to the temperatures of 300 ° C(Fig. 3b). Per-fect pseudoelasticity occurs between 255 ° C and 300 °C. For this particular aging treatment, the $Ni_{50.6}Ti_{34.4}Hf_{25.0}$ alloy also displays local perfect pseudoelasticity, e.g. at the test temperature of 270 °C we measured over the entire DIC region a maximum average strain of $\bar{\varepsilon} = 1.89\%$ and negligible residual strains, while locally we measured an average local strain of $\varepsilon_{loc} = 3.67\%$ and a residual strain of $\varepsilon^{res}_{loc} = 0.11\%$. Unrecovered residual plastic strains appear at temperatures higher than 315 °C. Aging at 400 °C for 4 h produces shape memory behavior (Fig. 3c). In the test temperature range (190–220)°C, the residual strains are completely recovered upon heating at zero stress above the A_F temperature.

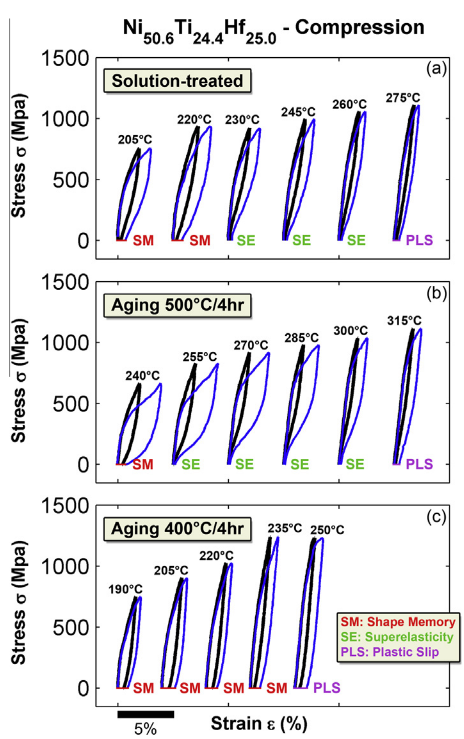

Figure 3. Influence of the aging temperature and test temperature on the isothermal behavior of the $Ni_{50.6}Ti_{24.4}Hf_{25.0}$ alloy under compression. Aging at 500 °C/4 h leads to superelasticity at higher temperatures (between 255 and 300 °C) than the solution-treated case, while aging at 400 °C/4 h inhibits the pseudoelasticity.

The superelastic behavior of the 500 °C/4 h aged specimen was further investigated by loading the specimen at different stress levels in a multiple load-step experiment at the test temperature of 265 ° C. Figure 4 shows the four stress–strain curves along with the DIC strain measurements captured during each of the load steps. The strain maps reported refer to the axial strains in the load direction. During load step A the maximum stress was $\sigma^{A}_{max} = 821$ Mpa and the maximum average axial strain was $\sigma^{A}_{max} = 2.25\%$. During the same load step A, locally the $Ni_{50.6}Ti_{34.4}Hf_{25.0}$ alloy shows strains up to $\varepsilon^{A,loc}_{max} = 4.11\%$ which were fully recovered $\varepsilon^{A,loc}_{max} = 0.08\%$ upon unloading. During the second load step B, the maximum stress reached $\sigma^{B}_{max} = 907$ Mpa with an average axial strain of $\sigma^{B}_{max} = 2.56\%$. Locally, the strains are extremely high, $\varepsilon^{A,loc}_{max} = 4.58\%$ and upon loading only a negligible residual strain is measured $\varepsilon^{A,loc}_{res} = 0.13\%$. With further load steps, residual strains or onset of instability develops. Additional experiments (herein omitted for brevity) show that the average failure strain is $\varepsilon_{failure} = 3.91\%$ with strain localization up to $\varepsilon^{loc}_{failure} = 6.01\%$.

In summary, we presented preliminary results on the characterization of the new high-temperature shape memory $Ni_{50.6}Ti_{34.4}Hf_{25.0}$ alloy. Transformation temperatures were determined for different combinations of aging temperatures and times. Stress–strain curves were then obtained for temperatures close to the austenite peak tem-perature (A_{PT}) for the solution-treated material, and for two different aging conditions: 400 °C/4 h and 500 °C/4 h. As expected [18], the precipitation by aging shifts the trans-formation temperatures to high temperatures. For the pres-ent $Ni_{50.6}Ti_{34.4}Hf_{25.0}$ alloy, aging temperatures higher than 500 ° C combined with a minimum aging time of 1 h set conditions that differ considerably from the solution-treated case (Fig. 2). In addition to this we observe that with aging in the temperature interval (400–500)°C the peak-to-peak difference ($A_{PT}-M_{TP}$) displays a minima of 29 ° C corresponding to 500 °C/4 h aging case. Moreover we also note for the 400 ° C/4 h aging a degradation of the superelastic response suggesting that a minimum aging temperature of 500 °C and a minimum aging time of 1 h are necessary in order to maximize the superelastic behavior of the $Ni_{50.6}Ti_{34.4}Hf_{25.0}$ alloy. A similar decrease in the transformation temperature for short-term aging between 450 ° C and 500 ° C was already observed for the $NiTiHf_{15}$ alloy [16,25] and explained with the small interparticle spacing induced by fine precipitates.

Near perfect superelastic behavior was obtained with 500 °C/4 h aging for specimens tested in the temperature range (255–300)°C. These temperatures exceed the observations of superelasticity in the literature at lower temperatures. At a temperature of 265 °C average local strains of 4.11% (maximum local transformation strains of 3.25%) at a maximum stress of 821 MPa were fully recovered upon unloading (Fig. 4). In perspective, the measurement of such high local strains is promising for future research on the

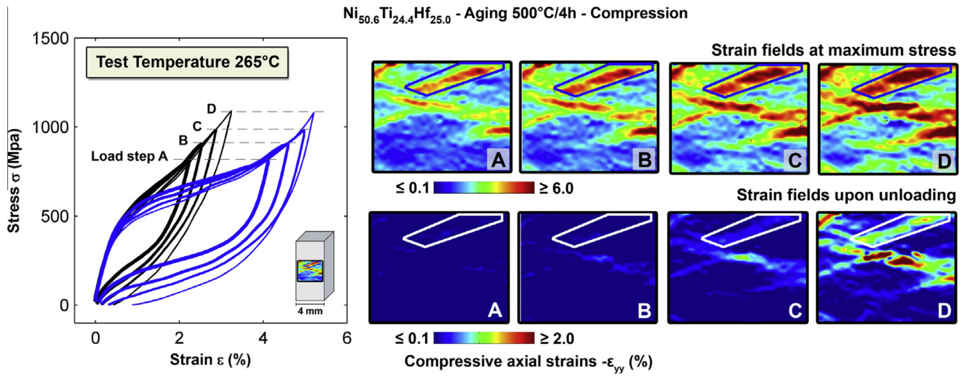

Figure 4. Influence of the maximum applied stress for the $Ni_{50.6}Ti_{24.4}Hf_{25.0}$ alloy aged at 500 °C/4 h and tested at 265 °C under compression at a strain rate of $2.7{\cdot}10^{-4}\,s^{-1}$. Local in situ DIC strain measurements (blue curve) show a complete local strain recovery during load step A ($\varepsilon^{max}_{A,loc} = 4.11\%$). DIC strain fields indicate the increment of the irrecoverable strain with the applied stress from load step B. (For interpretation of the references to color in this figure legend, the reader is referred to the web version of this article.)

$Ni_{50.6}Ti_{34.4}Hf_{25.0}$ single crystals. Superelastic behavior was also observed for the solution-treated case, while aging at 400 °C/4 h suppressed the superelastic response. Preliminary results on higher aging temperatures (not reported here for brevity) show that also with further increasing the aging temperature over 600 °C the superelasticity is partially inhibited. These results indicate that the calibration of NiTiHf alloys for obtaining the desired shape memory and superelastic behaviors requires the definition of an optimum aging temperature. The choice of the correct aging temperature and time has to consider the type of precipitate (composition and coherency of the precipitate), the size and the interparticle distance since these parameters strongly influence the transformation temperatures and the functionality of NiTiHf alloys. Further analyses will provide insights for the preliminary observations reported.

The work was supported by NSF-CMMI 1333884 which is gratefully acknowledged.

[1] J. Ma, I. Karaman, R.D. Noebe, Int. Mater. Rev. 55 (2010) 257–315.
[2] D.N. AbuJudon, P.E. Thoma, M.-Y. Kao, D.R. Angst, High transformation temperature shape memory alloys, US patent, 1992.
[3] D.R. Angst, P.E. Thoma, M.Y. Kao, The effect of hafnium content on the transformation temperatures of Ni[49]Ti[51-x] Hf[x] shape memory alloys, EDP sciences, Les Ulis, France, 1995.
[4] S. Besseghini, E. Villa, A. Tuissi, Mater. Sci. Eng. A 273–275 (1999) 390–394.
[5] B. Kockar, I. Karaman, J.I. Kim, Y. Chumlyakov, Scr. Mater. 54 (2006) 2203–2208.
[6] P. Thoma, E.C. Zhang, J. Boehm, J.R. Zee, J. Phys. IV 07 (1997) C5483–C5488, France.
[7] X.D. Han, R. Wang, Z. Zhang, D.Z. Yang, Acta Mater. 46 (1998) 273–281.
[8] Y.F. Zheng, L.C. Zhao, H.Q. Ye, Scr. Mater. 38 (1998) 1249–1253.
[9] Y.Q. Wang, Y.F. Zheng, W. Cai, L.C. Zhao, Scr. Mater. 40 (1999) 1327–1331.
[10] X.L. Meng, Y.F. Zheng, Z. Wang, L.C. Zhao, Scr. Mater. 42 (2000) 341–348.
[11] M. Moshref-Javadi, S.H. Seyedein, M.T. Salehi, M.R. Aboutalebi, Acta Mater. 61 (2013) 2583–2594.
[12] G.S. Bigelow, A. Garg, S.A. Padula Ii, D.J. Gaydosh, R.D. Noebe, Scr. Mater. 64 (2011) 725–728.
[13] W. Cai, X.L. Meng, L.C. Zhao, Curr. Opin. Solid State Mater. Sci. 9 (2005) 296–302.
[14] D.R. Coughlin, P.J. Phillips, G.S. Bigelow, A. Garg, R.D. Noebe, M.J. Mills, Scr. Mater. 67 (2012) 112–115.
[15] H.E. Karaca, S.M. Saghaian, B. Basaran, G.S. Bigelow, R.D. Noebe, Y.I. Chumlyakov, Scr. Mater. 65 (2011) 577–580.
[16] H.E. Karaca, S.M. Saghaian, G. Ded, H. Tobe, B. Basaran, H.J. Maier, R.D. Noebe, Y.I. Chumlyakov, Acta Mater. 61 (2013) 7422–7431.
[17] X.L. Meng, W. Cai, Y.D. Fu, Q.F. Li, J.X. Zhang, L.C. Zhao, Intermetallics 16 (2008) 698–705.
[18] X.L. Meng, W. Cai, Y.F. Zheng, L.C. Zhao, Mater. Sci. Eng. A 438–440 (2006) 666–670.
[19] R. Santamarta, R. Arróyave, J. Pons, A. Evirgen, I. Karaman, H.E. Karaca, R.D. Noebe, Acta Mater. 61 (2013) 6191–6206.
[20] F. Yang, D.R. Coughlin, P.J. Phillips, L. Yang, A. Devaraj, L. Kovarik, R.D. Noebe, M.J. Mills, Acta Mater. 61 (2013) 3335–3346.
[21] S.-H. Kang, T.-H. Nam, Met. Mater. Int. 7 (2001) 443–446.
[22] S. Sanjabi, Y.Z. Cao, Z.H. Barber, Sens. Actuators A 121 (2005) 543–548.
[23] Y. Tong, Y. Liu, J. Miao, Thin Solid Films 516 (2008) 5393–5396.
[24] O. Benafan, A. Garg, R.D. Noebe, G.S. Bigelow, S.A. Padula Ii, D.J. Gaydosh, N. Schell, J.H. Mabe, R. Vaidyanathan, Intermetallics 50 (2014) 94–107.
[25] A. Evirgen, F. Basner, I. Karaman, R.D. Noebe, J. Pons, R. Santamarta, Funct. Mater. Lett. 05 (2012) 1250038.